JOURNAL OF PHYSICAL ORGANIC CHEMISTRY, VOL. 10, 623–630 (1997)

ELECTRON TRANSFER PROPERTIES OF NON-ALTERNANT, SUBSTITUTED COMPOUNDS RELATED TO FLUORANTHENE. EXPERIMENTAL DETERMINATION AND THEORETICAL MODELING OF ELECTROCHEMICAL OXIDATION AND REDUCTION POTENTIALS IN NON-AQUEOUS SOLUTION

L. KRAIG STEFFEN,[1]* BENJAMIN F. PLUMMER,[2] TALA L. BRALEY,[1] W. GREG REESE,[1] KATHRYN ZYCH,[1] GREGORY VAN DYKE[1] AND MICHAEL GILL[1]

[1]*Department of Chemistry, Fairfield University, Fairfield, Connecticut 06430, USA*
[2]*Department of Chemistry, Trinity University, San Antonio, Texas 78212, USA*

The oxidation and reduction potentials of a series of related even non-alternant derivatives of 7,14-disubstituted acenaphth[1,2-*k*] fluoranthenes, and also fluoranthene, 7,10-diphenylfluoranthene and 8,9-dihydrodiindeno[1,2-*j*;2′,1′-] fluoranthene, were determined in organic solvents by cyclic voltammetry. The effects of steric hindrance on conjugation of the substituents with the central polycyclic aromatic hydrocarbon nucleus were evaluated. The semi-empirical molecular orbital calculation programs OMEGAMO, Extended Hückel, AM1 and PM3 were used to obtain optimal geometries and calculated HOMO and LUMO energies. As a further refinement, COSMO solvation was included in the AM1 calculations. The redox properties were correlated with data derived from the various semi-empirical calculations and the quality of these correlations is discussed. Inclusion of solvation energies in the computed molecular orbital energies results in a significant improvement in the correlation between observed and calculated oxidation potentials.

J. Phys. Org. Chem. **10**, 623–630 (1997) No. of Figures: 7 No. of Tables: 3 No. of References: 28
Keywords: Electron transfer properties; substituted flouranthene derivatives; redox potentials
Received 22 November 1996; revised 25 February 1997; accepted 6 March 1997

INTRODUCTION

Cyclopentene-fused polycyclic aromatic hydrocarbons (CPAH) occur in the environment as the result of combustion of petroleum-based fuels. Many are of concern owing to their carcinogenicity. These compounds have received renewed interest because the techniques of flash vacuum thermolysis have allowed the synthesis of new compounds whose chemistry is unexplored.[1] A broader understanding of the chemistry of buckminsterfullerene, a CPAH, may also be reflected in studies of simpler CPAH. The reactivity of even, non-alternant CPAH is frequently different from that of even alternant PAH.[2,3] Also, fusion of a benzenoid PAH to a five-membered ring introduces steric strain.[4] This study is presented because the chemistry of these non-alternant hydrocarbons and their substituted compounds is sparsely documented.

A series of substituted fluoranthene derivatives (Scheme 1) was studied because they contain aryl groups with significantly decreased conjugation caused by steric inhibition of resonance. X-ray crystallographic data clearly show that the substituents are constrained to a geometry essentially perpendicular to the molecular plane of the PAH core in **1b**, **11** and **2b**.[5] Fluorescence stead-state and lifetime emission studies of these compounds showed that altering substituents at the 7,14-positions of the acenaphth[1,2-*k*]fluoranthenes causes only small changes in the emission spectra, irrespective of the type of substituent. This indicates that the phenyl and carbethoxy substituents bonded to the 7,14-positions are not capable of significant

Correspondence to: L. K. Steffen. E-mail: 1steffen@fair1.fairfield.edu.
Contract grant sponsor: NSF; *Contract grant number*: CHE-8922685; *Contract grant number*: CHE-9224324.
Contract grant sponsor: Camille and Henry Dreyfus Foundation

 CCC 0894–3230/97/080623–08 $17.50

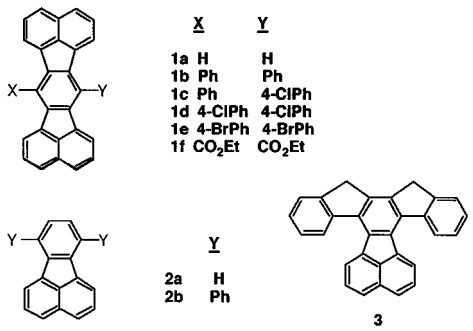

Scheme 1

direct resonance interaction with the central CPAH. Strong evidence for the modulation of the resonance effect in these compounds is seen in the moderation of the heavy atom quenching of their fluorescence.[7]

The ease with which electrons can be added to or removed from the CPAH provides a direct probe of their reactivity and can provide additional information about substituent effects. Semi-empirical molecular orbital calculations can be used to determine the energies and nodal properties of the HOMO and LUMO of each compound. These results can then be used to correlate the effect of substituents on the stabilization of charged species and to test assumptions about the behavior of non-alternant CPAH. Equilibrium oxidation and reduction potentials ($E^{\circ\prime}$), obtained from polarography or cyclic voltammetry, provide direct thermodynamic information about the ease of removal from or addition of electrons to PAH. The potentials for even alternant PAH have been correlated with the energies of the HOMO[8] and LUMO,[9] ionization potentials,[10] electron affinities and charge transfer band energies.[11] Most electrochemical studies have been performed on simple PAH or on those containing only alkyl or aryl substituents. Few studies exist for substituted PAH that contain heteroatom substituents.

Work has been done on anthracene derivatives[12] using cyclic voltammetry that provides evidence for the relative stabilities of the cation and anion radicals as measured by their reversible formation.[13] For a reversible oxidation, the relationship between the oxidation potential and the HOMO energy expressed as the ionization potential is

$$E^{\circ\prime} = IP + \Delta E(\text{sol}) - T\Delta S/F - (RT/F)\ln(f^{+}D^{+}/FD) \times \text{constant} \quad (1)$$

where IP is the ionization potential, ΔE(sol) is the difference in solvation energy between the neutral compound and its cation radical, D and D^{+} are the diffusion coefficients for the neutral and charged species, respectively, and f and f^{+} are the corresponding activity coefficients. For large PAH, the ΔE(solv) term is ordinarily assumed to be small and similar in magnitude within a series of similar structures. However, the validity of this assumption is suspect for non-alternant substituted CPAH. We have addressed this issue by use of a calculation that includes solvation. The program COSMO is a continuum solvation model that calculates the energy for irregularly shaped solutes and solvents of varying dielectric properties.[14] COSMO has proven useful for the modeling of other redox systems, such as quinones.[15] Previous arguments[8] assumed that upon transformation from the neutral to the charged molecule the diffusion coefficient decreases and the activity coefficient increases proportionately so that a negligible logarithmic term is obtained. The validity of this assumption for even non-alternant CPAH remains unproven. Azulene and acenaphthylene represent two examples of non-alternant PAH studied previously and their oxidation potentials did not correlate well with the calculated energy of the HOMO. Extra aromatic stabilization available to polar resonance structures of the cation radicals of azulene and acenaphthylene was invoked as the reason that these two compounds deviated from the correlation. These polar resonance forms were theorized to cause a significant difference in the ΔE(sol) term, which led to a poor correlation. A simple relationship between the reduction potential and the energy of the LUMO:

$$-E^{\circ\prime} = A/F + C \quad (2)$$

was also applied to even-alternant PAH using similar assumptions. The electron affinity, A, corresponds to the energy of the LUMO in eV, F is the Faraday and C is a constant that includes terms similar to those described in equation (1). An attempt was made to correlate the reduction potentials with the simple Hückel LUMO energies of a limited number of sterically constrained, even alternant PAH.[16] The correlation was significantly improved by use of a more sophisticated Hückel program, OMEGAMO.[17] Similar assumptions about rates of diffusion, activity coefficients and solvation effects in the oxidations were also used to derive equation (2) and thus similar concerns about generality are raised. In this paper, the oxidation and reduction potentials of compounds related to fluoranthene (Scheme 1) are compared with values calculated from semi-empirical calculations of the HOMO and LUMO energies using OMEGAMO, Extended Hückel, PM3, AM1 and AM1 with COSMO solvation.

EXPERIMENTAL

General. ^{1}H NMR spectra were obtained on a Varian VXR-300 spectrometer at 300 MHz, using $CDCl_3$ solutions with internal tetramethylsilane (TMS). Melting points were determined on a Meltemp apparatus and are uncorrected. IR spectra were obtained as KBr pellets on a Perkin-Elmer Model 1600 FT-IR instrument. Mass spectra were determined by direct insertion on a Hewlett-Packard Model 5995-C GC mass spectrometer at 70 eV ionizing radiation. Elemental analyses were performed by Texas Analytical Laboratories. The methods and procedures used for the cyclic voltammetry are as described previously.[8]

Calculations. A suite of computational programs was used to analyze the orbital energies and geometries of the molecules under investigation. Orbital energies were calculated using two Hückel MO programs, OMEGAMO[9] and Extended Hückel,[18] by PM3[19] and AM1[20] semi-empirical calculations and, finally, AM1 with COSMO[14] solvation. Except for OMEGAMO, all of the programs used were implemented as part of the CAChe[21] molecular modeling environment.

Syntheses. Fluoranthene was used as obtained from Aldrich. Compounds **1a**,[22] **2b**,[23] **1b**,[24] **1f**[22] and **3**[25] were synthesized according to literature procedures. Acecyclone and its substituted aryl derivatives were prepared according to literature procedures.[25,26]

7-(4-Chlorophenyl)-14-phenylacenaphth[1,2-k]fluoranthene (*1c*). Into a 250 ml round-bottomed flask fitted with a reflux condenser and magnetic stirrer containing a solution of 1-bromoacenaphthylene (1·3 g, 5·5 mmol) and xylenes (25 ml) was added 4-chlorophenylphenylacecyclone (2·0 g, 5·0 mmol) and the solution was refluxed for 52 h. When evolution of HBr was negligible the solution was cooled to 0 °C and the yellow solid was collected by vacuum filtration to produce 0·5 g of material. The solid was dissolved in 50% THF–methanol (300 ml) and the resulting green solution was treated with $NaBH_4$ (0·2 g) to reduce unreacted cyclone. Addition of water (50 ml) caused the precipitation of a yellow solid (0·5 g, 19%), m.p. 343–346 °C; ^{1}H NMR ($CDCl_3$, 300 MHz), δ=7·65–7·78 (m, 7, ArH), 7·4 (dd, 1, J=8·2, 7·2 Hz, H5), 7·37 (dd, 1,J=8·2, 7·2 Hz, H2), 6·81 (d, 1, J=7·2 Hz, H1), 6·76 (d, 1, J=7·2 Hz, H6), 7·76 (dd, 1, J=8·5, 0·5 Hz, H3), 7·73 (d, 1,J=8·1 Hz, H4), 7·63 (d, 1, J=8·1 Hz, H5), 7·39 (dd, 1,J=8·1, 7·1 Hz, H2), 6·74 (d, 1, J=7·1 Hz, H1). Analysis: calculated for $C_{38}H_{21}Cl$, C 88·96, H 4·13, Cl 6·91; found, C 89·26, H 4·15, Cl 6·96%.

7,14-Bis(4-chlorophenyl)acenaphth[1,2-k]fluoranthene (*1d*). Into a 100 ml round-bottomed flask fitted with a reflux condenser and magnetic stirrer containing a solution of 1-bromoacenaphthylene (0·5 g, 1·9 mmol) and xylenes (25 ml) was added bis(4-chlorophenyl)acecyclone (0·7 g 1·6 mmol) and the solution was refluxed for 24 h. When evolution of HBr was negligible the solution was cooled and the xylenes were removed by rotary evaporation. The tarry product was dissolved in 50% methylene chloride–cyclohexane (30 ml) and filtered through a layer of active alumina on a Buchner funnel. The filtrate was rotary evaporated to yield a yellow solid that was recrystallized from methylene chloride–cyclohexane (1:1) to yield 0·5 g of product (71%), m.p. >350 °C (decomp.); ^{1}H NMR ($CDCl_3$, 300 mHz), δ=7·76 (dd, 1, J=8·5, 0·5 Hz, H3), 7·73 (d, 1, J= 8·1 Hz, *m*-phenyl), 7·63 (d, 1, J=8·1 Hz, *o*-phenyl, 7·39, (dd, 1, J=8·1, 7·1 Hz, H2), 6·74 (d, 1, J=7·1 Hz, H1). Analysis: calculated for C_{38} for $C_{38}H_{20}Cl_2$, C 83·36, H 3·68, Cl 12·95; found, C 83·59, H 3·70, Cl 12·85%.

7,14-Bis(4-bromophenyl)acenaphth[1,2-k]fluoranthene (*1e*). Into a 100 ml round-bottomed flask fitted with a reflux condenser and magnetic stirrer containing a solution of 1-bromoacenaphthylene (0·9 g, 3·8 mmol) and xylenes (25 ml) was added dibromo *p*,*p*′-diphenylacecyclone (1·35 g, 2·62 mmol) and the solution was boiled at reflux for 2·5 days. After cooling overnight at 0 °C, insoluble acecyclone was removed by gravity filtration and the solid rinsed with warm xylenes (50 ml). The xylenes were removed by rotary evaporation and the resulting brown solid was recrystallized from toluene to give yellow crystals (0·43 g, 26%), m.p.>400 °C; ^{1}H NMR ($CDCl_3$, 300 MHz), δ=7·89 (d, 1, J=8·3 Hz, *m*-phenyl), 7·78 (d, 1, J=7·8 Hz, H3), 7·58 (d, 1, J=8·3 Hz, *o*-phenyl), 7·40 (dd, 1, J=8·3, 7·2 Hz, H2), 6·79 (d, 1,J=7·2 Hz, H1). Analysis: calculated for $C_{38}H_{20}Br_2$, C 71·74, H 3·14, Br 25·12; found, C 71·48, H 3·18, Br 25·02%.

RESULTS

Oxidations

Oxidation peak potentials (E_{pa}) are given and $E^{\circ\prime}$ values are given for those compounds that exhibited reversible oxidation (Table 1). The mixed solvent system of methylene chloride–trifluoroacetic acid–trifluoroacetic anhydride has been shown to be an excellent solvent for the generation of cationic species.[27] Trace amounts of water, which can react with cation radicals, are scavenged effectively by this mixture and the cation radicals may also be stabilized by ion-pair interaction with the trifluoroacetate. After correcting for differences in the reference electrode and comparing the data available[28] for fluoranthene and anthracene, it is apparent that, in this solvent system, the E_{pa} values are shifted anodically by about 160 mV. This does not affect the conclusions derived from this study because relative oxidation potentials are compared. Reversibility was judged by a number of criteria. At 100 mV^{-1} s the ratio of the anodic and cathodic peak currents was close or equal to 1. The peak potential shifted by less than 20 mV as the scan rate was increased from 20 to 800 mV s^{-1}. The separation between the anodic and cathodic peaks was 80–110 mV. While the occurrence of a chemical reaction cannot be dismissed, the larger than theoretical peak separation is probably due to the relatively low-polarity solvent mixture used. All of the compounds produced diffusion-controlled oxidations as indicated by linear plots of the square root of the sweep rate versus the anodic peak current.

Reductions

All of the compounds studied showed reversible reductions so $E^{\circ\prime}$ values are reported in addition to the E_{pc} values

Table 1. Electrochemical data

Compound	E_p (Ox) (V)[a]	$E°$ (Ox) (V)	E_p (Red) (V)[b]	$E°$ (Red) (V)
1a	1·060	1·020	−1·513	−1·457
1b	1·119	1·079	−1·655	−1·609
1c			−1·398	−1·368
1d	1·169	1·119	−1·375	−1·339
1e	1·203	1·150	−1·710	−1·670
1f	1·426		−1·269	−1·218
2a	1·360		−1·730	−1·680
2b	1·238		−1·641	−1·610
3	0·933	0·891	−1·616	−1·570
Ferrocene		0·080		

[a] Volts vs Ag/0·1 M $AgNO_3$ in ACN. Solution is 8:1·5:0·5 ACN–TFA–TFAA.
[b] Volts vs Ag/AgCl (aq.) in DMF. Pt working and counter electrodes. 100 mV^{-1} s. *Ca* 10^{-3} M in compound.

(Table 1). The criterion for reversibility of the oxidations was applied to the reductions. For the reductions the measured value for fluoranthene is only 25 mV cathodic from that reported by Hoijtink[16] when corrected for the difference in the reference electrode used.

Calculations

The calculated orbital energies are summarized in Table 2. Energy-minimized structures using AM1 and PM3 were obtained for all of the molecules. Space-filling models using the PM3 geometry are shown for **1b**, **1f**, **2b** and **3** (Figure 1). In 7,10-diphenylfluoranthene (**2b**), the π-bonded phenyls can distort upwards and can rotate about +20° around the dihedral before encountering significant steric strain from the buttressing hydrogens.[7] The PM3 calculations indicate that the phenyls are twisted about 8° in the minimum energy conformation. In the series **1b–e** the π-bonded phenyls are held near 90° around the dihedral. In **3** the phenyls are constrained by the bridging methylenes to a nearly planar geometry with respect to the fluoranthene plane, resulting in significant steric strain. In **3** the phenyls are computed to distort symmetrically on either side of the fluoranthene nucleus. An alternative conformation in which both phenyls are bent into a U-shape was calculated to be slightly higher in energy. HOMO and LUMO diagrams for **1b**, **2a**, **2b** and **3** have been published (Figure 9 in Ref. 7). The HOMO of **1b** is comprised mostly of π-type overlap of p-orbitals on the central acenaphth[1,2-*k*]fluoranthene frame. No significant π-type overlap with the phenyl substituent p-orbitals is seen. However, there is a small calculated contribution to the HOMO by the *s*-bonds of the attached phenyls. This unusual overlap is a direct consequence of the steric constraints placed upon **1b** by the buttressing hydrogens and is similar to that seen with perpendicular overlap of cyclopropane conjugated with a carbocation. The HOMOs for **1c–e** are very similar to that shown for **1b** and as the substituent is changed from H to Br the coefficients for the σ-type overlap increase slightly. The LUMOs of **1a–f** all have a node at the 7,14-positions and show no contribution from the substituents. In the HOMO of **2b**, there is a greater contribution from the substituent phenyls and it is a mixture of the σ-type overlap seen for **1b** and a small amount of π-type overlap. The coefficient for the p_z-orbital at the carbon attached to the central ring system is proportionally larger for **2b** than **1b**. In **3**, where the bridging methylenes force the phenyls closer to planarity, the HOMO shows a large π-type overlap

Table 2. Computed molecular orbital energies

Compound	OMEGAMO (β)	Extended Hückel (β)	PM3 (eV)		AM1 (eV)		AM1 solv. (eV)	
	LUMO	LUMO	LUMO	HOMO	LUMO	HOMO	LUMO	HOMO
1a	0·354	0·341	−1·397	−8·698	−1·39213	−8·4126	−1·57940	−8·66068
1b	0·353	0·341	−1·378	−8·384	−1·23763	−8·30176	−1·44209	−8·56579
1c	0·356	0·341	−1·403	—	−1·30413	—	−1·47870	—
1d	0·358	0·341	−1·448	−8·505	−1·37075	−8·43923	−1·51452	−8·63533
1e	0·360	0·341	−1·480	−8·540	−1·39294	−8·46437	−1·52793	−8·64904
1f	0·357	0·341	−1·474	−8·365	−1·52941	−8·66396	−1·82961	−8·94427
2a	0·444	0·489	−1·061	−8·698	−0·92943	−8·62992	−1·17768	−8·86446
2b	0·436	0·327	−1·011	−8·633	−0·89966	−8·45808	−1·07167	−8·68848
3	0·436	0·327	−1·074	−8·254	−0·94781	−8·1261	−1·21866	−8·40479

contribution from the phenyls. In **3**, the LUMO-s also show no significant contribution from the phenyls. Crystallographic data for **2b**,[5] **1b** and **1f**[6] support the computational results. The x-ray results show that the substituents are twisted far out of the plane, 70° for **2a** and 90° for **1b** and **1f**, and limited from rotating into the plane by *ortho*-protons.

DISCUSSION

Oxidations

The oxidation potentials are modeled best by the AM1 Hamiltonian (Figure 2, $r = 0{\cdot}90$). Both AM1 and PM3 correlated the oxidation potential of **1a** poorly, calculating a HOMO energy much lower (harder to oxidize) than that expected based upon the electrochemical data. The diester, **1f**, also deviates substantially when PM3 is used, but a better correlation occurs with AM1.

A significant increase in the quality of the correlation is observed when solvation was modeled using the conductor-like screening model (COSMO). COSMO is a dielectric continuum model which allows for irregularly shaped solutes and solvents of varying polarity. A polar solute creates a polarized cavity, defined by a solvent-accessible surface (SAS), which perturbs the surrounding dielectric. The effect of the solvent polarity on the electronic properties of the solutes can then be modeled by integrating the effect of the solvent over the entire surface by solution of an equation of the form

$$4\pi\varepsilon\sigma(r) = (\varepsilon - 1)n(r)E^{-}(r) \tag{3}$$

where ε is the permittivity of the dielectric, $\sigma(r)$ is the screening charge density, $n(r)$ is the surface normal vector at a particular point on the solute (r) and $E^{-}(r)$ represents the total electric field on the inner surface of the SAS at one point. Although simple in form, calculation of the screening charge densities with real molecules is complicated by the fact that few have simple, smooth SASs. In COSMO, equation (3) is solved using an approach based on the screening of conductors which allows for an approximate but theoretically very accurate solution. Since the electrochemical solution used was a mixture, the solvation for the CPAH was modeled by using an average of solvent radii and dielectric for methylene chloride and trifluoracetic acid. [The average solvent radius used was 9·00 Å. COSMO actually uses a solvent radius value less than the actual radius which corrects for the ability of charge to polarize within the solvent. Use of the default value for R_{solv} gave slightly poorer results. The average dielectric was approximated as 9·5 D. Dielectric constants are not truly additive whereas susceptibilities ($\varepsilon - 1$) are. Use of an average susceptibility expressed as a dielectric changed the energy

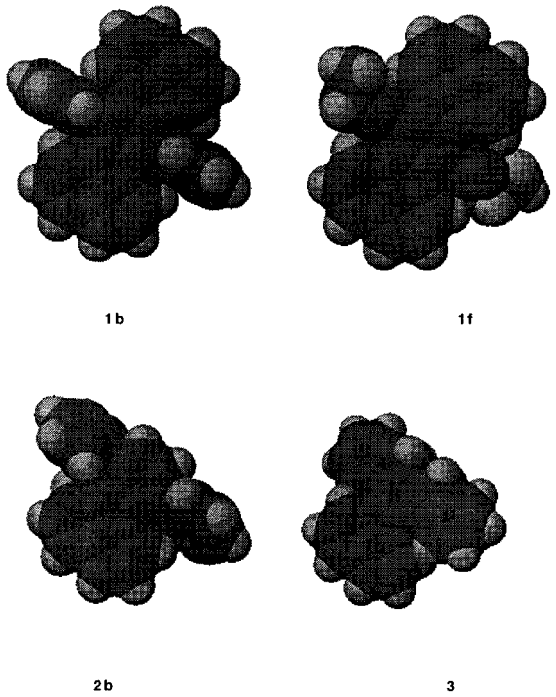

Figure 1. Space filling models of **1b**, **1f**, **2b** and **3** which illustrate the steric interactions in the molecules. Lowest energy conformations from AM1 calculations. See Ref. 7 for modeling of these interactions

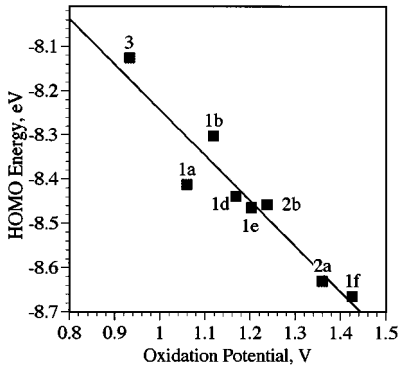

Figure 2. Correlation between electrochemical oxidation peak potentials and the calculated HOMO energy from AM1 ($r = 0{\cdot}90$)

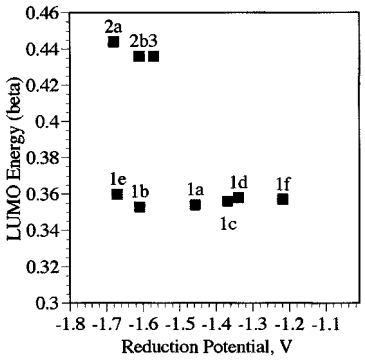

Figure 4. Attempted correlation between electrochemical reduction peak potentials and the calculated LUMOβ energy from OMEGAMO

obtained by a very small amount and so the original approximation was used. It is recognized that the presence of significant amounts of supporting electrolyte effectively increases the dielectric constant of the solution. This problem will be the subject of future theoretical work. An improved correlation is obtained ($r = 0{\cdot}984$, Figure 3), indicating that COSMO is capable of accounting for the solvation changes, even at the lower dielectric values. The observed trends are in accord with what would be expected based upon resonance and inductive influences of the substituents. For example, **1f**, with a carbonyl directly attached to the PAH core, exerts a strong inductive effect causing **1f** to be much harder to oxidize. Likewise, the halogen substituents, moderated by a phenyl group, exert a small inductive shift in the oxidation potential which is reflected in the ground state HOMO energy. One critical note is that compound **1a** was again far off the line and it was therefore not included. The reason for its failure to correlate is under investigation. The progression from **2a** to **2b** to **1b** clearly shows the effect of increasing the size of the central PAH core. Compound **3** exhibits a lowering of its oxidation potential due to increased conjugation of the attached phenyls and a significant decrease due to steric strain. It is encouraging that the modeling programs were able to predict accurately the decreased oxidation potential of **3**. The oxidation results are also in accord with the

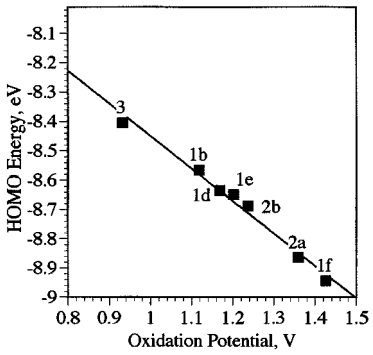

Figure 3. Correlation between electrochemical oxidation peak potentials and the calculated HOMO energy from AM1 with COSMO solvation of ACN–trifluoracetic acid included ($r = 0{\cdot}98$)

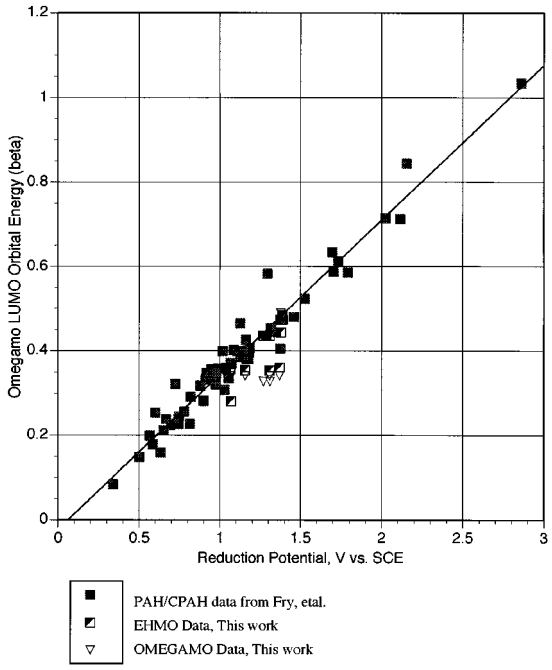

Figure 5. OMEGAMO data for the Compounds in Scheme 1 embedded in a larger set of data for which OMEGAMO calculations were successful

Table 3. Charge-transfer bands of selected compounds complexed with TCNE[a]

Compound	HOMO–LUMO gap (eV)	CT band (cm^{-1})
1a	7·02047	15480
1b	7·06413	15243
1f	7·13455	17422
2a	7·70049	18051
2b	7·55842	17606

[a] 10^{-3} M donor complexed with 10^{-2} M TCNE in CH_2Cl_2.

computed HOMO energies, since these indicate that the 4-X-phenyl substituents when attached to the central PAH core perturb the energies of the molecules by an electron-withdrawing inductive effect. The slope for Figure 3 is near -1, which indicates that the solvated HOMO calculations can serve as a useful predictor of actual oxidation potentials, not just trends in those potentials.

Reductions

The measured reduction potentials are not modeled as well. Based on earlier work,[9] the reductions were correlated with LUMO energies obtained by use of the modified Hückel program, OMEGAMO (Figure 4). Clearly, despite an observed shift in the reduction potentials of over 400 mV, the computation was effectively insensitive to substituent perturbations. As expected, OMEGAMO was sensitive to large differences in the total amount of π-delocalization because **2a** and **2b** were both calculated to be harder to reduce than **1a** and **1b**. Using OMEGAMO, the parameters for substituents were varied and a dihedral angle correction for orbital overlap of attached phenyls was implemented. The poor correlations obtained are not surprising. Maximum overlap of the phenyl substituents was initially assumed, which is unlikely for **1a**–**e**. Our data derived from

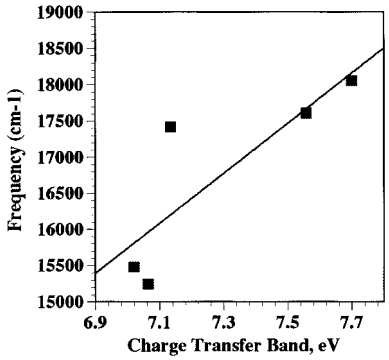

Figure 6. Correlation between the HOMO–LUMO gap by AM1 and the energy of the charge-transfer band for selected complexes with TCNE ($r = 0{\cdot}67$)

OMEGAMO are illustrated embedded in a larger data set for which OMEGAMO gave reasonable results (Figure 5). When the Extended Hückel method was used for calculating the LUMO energies, a poor correlation also resulted. Similarly, if the PM3 Hamiltonian is used, the correlation with the reduction potentials is again poor. AM1 calculations show a modest correlation which improves slightly when solvation with DMF, modeled by COSMO, is included. Because the calculations indicate a node in the LUMO at the 7,14-positions for **1b**–**f**, it is not surprising that the calculations of reduction potentials were relatively insensitive to substitution on the attached phenyls. AM1 data for the SOMO energy of the anion radicals on a subset of the compounds also did not indicate a significant improvement over that observed with the LUMOs. Clearly, for the reductions, the level of computational theory applied was not sufficient to discern the trends observed.

Since data were also available on the charge-transfer bands observed for **1a**, **1b**, **1f**, **2a** and **2b** when complexed with TCNE in methylene chloride, these were compared with the HOMO–LUMO gap calculated by AM1. The general trend observed is as expected. The compounds with greater π-type overlap between phenyl substituents and the central CPAH core showed a longer wavelength CT band, but the correlation was again modest (Table 3, Figure 6).

CONCLUSIONS

The oxidation and reduction potentials of a related series of even, non-alternant fluoranthene derivatives were determined in mixed organic solvents. Most of the compounds exhibited reversible or quasi-reversible cyclic voltammograms under the conditions used, with the exception of the irreversible oxidation of **2a** and **2b**. Semi-empirical MO calculations of the HOMO energies for the series correlated well with the oxidation potentials, especially when solvation, modeled by COSMO, was included. The calculated energies of the LUMO produced a poor correlation with the experimentally determined reduction potentials irrespective of the semi-empirical program chosen. Calculated energy changes for the HOMO as a function of substituents and variations in the experimentally determined oxidation and reduction potentials were consistent with inductive effects for the majority of compounds in the series. The poor correlation found for the LUMO energies with the reduction potentials suggests that there may be significant differences in the solvation energies of the different radical anions that are formed. It is clear that more work is needed to understand substituent and solvent effects on CPAH.

ACKNOWLEDGMENTS

The NSF, through Grants CHE-8922685 and CHE-9224324, and the Camille and Henry Dreyfus Foundation are thanked for their support of this research.

REFERENCES

1. L. T. Scott and A. Necula, *J. Org. Chem.* **61**, 386–388 (1996), and references cited therein.
2. B. F. Plummer and S. F. Singleton, *Tetrahedron Lett.* **28**, 4801–4804 (1987).
3. B. F. Plummer and S. F. Singleton, *J. Phys. Chem.* **93**, 5515–5520 (1989).
4. R. H. Boyd, R. L. Christensen and R. Pua, *J. Am. Chem. Soc.* **87**, 3554–3559 (1965).
5. B. F. Plummer, W. G. Reese, W. H. Watson, and R. P. Kashyep, *Acta Crystallogr.*, **47**, 1848–1851 (1991).
6. B. F. Plummer, W. G. Reese, W. H. Watson and M. Krawiec, *Struct. Chem.* **4**, 53–57 (1993).
7. B. F. Plummer, L. K. Steffen, T. L. Braley, W. G. Reese, K. Zych, G. VanDyke and B. Tulley, *J. Am. Chem. Soc.* **115**, 11542–11551 (1993).
8. E. S. Pysh and N. C. Yang, *J. Am. Chem. Soc.* **85**, 2194 (1965).
9. A. Fry and P. C. Fox, *Tetrahedron* **42**, 5255–5266 (1986).
10. R. E. Cremonesi and E. Cavalieri, *Chem. Res. Toxicol.* **5**, 346–355 (1992).
11. J. M. Masnovi, E. A. Seddon and J. K. Kochi, *Can J. Chem.* **62**, 2252–2259 (1984).
12. E. Cheng, T. C. Sun and O. Y. Su, *J. Chin. Chem. Soc.* **40**, 551–555 (1993); A. Yildiz, *Chim. Acta Turc.* **4**, 211–225, (1976).
13. M. Peover and B. S. White, *Electroanal. Chem.* **13**, 93–99 (1967).
14. A. Klamt and G. Schuurmann, *J. Chem. Soc., Perkin Trans. 2* 799–805 (1993).
15. H. S. Rzepa and G. A. Suner, *J. Chem. Soc., Chem. Commun.* 1743–1744 (1993); M. Jalali-Heravi, M. Namazian and T. E. Peacock, *J. Electroanal. Chem.* **385**, 1–8 (1995).
16. G. J. Hoijtink, *Recl. Trav. Chim. Pays-Bas* **74**, 1525–1539 (1955).
17. G. J. Hoijtink, *Recl. Trav. Chim. Pays-Bas* **71**, 1089–1103 (1952).
18. J. P. Lowe, *Quantum Chemistry.* Academic Press, New York (1978).
19. J. J. P. Stewart, *J. Comput.-Aided Mol. Res.* **4**, 1 (1990).
20. M. J. S. Dewar, E. G. Zoebisch, E. F. Healy and J. J. P. Stewart, *J. Am. Chem. Soc.* **107**, 3902–3909 (1985).
21. *Computer Aided Chemistry Version 3.6.* CA Che Scientific, Beaverton, OR (1994).
22. S. H. Tucker, *J. Chem. Soc.* 1462–1463 (1958).
23. J. T. Craig and M. D. W. Robins, *Aust. J. Chem.* **21**, 2237–2245 (1968).
24. D. K. Ganajep, *Indian J. Chem.* **15B**, 953–955 (1977).
25. W. Dilthey and S. Henkels, *J. Prakt. Chem.* **85**, 85–97 (1937).
26. R. B. Pascal, W. P. McMillan, D. VanEngen and R. G. Eason, *J. Am. Chem. Soc.* **109**, 4660–4665 (1987).
27. O. Hammerich and V. D. Parker, *J. Am. Chem. Soc.* **93**, 4289–4290 (1974).
28. L. Meitas and P. Zuman, *Handbook Series in Organic Electrochemistry.* CRC Press, Cleveland, OH (1976).

